

# Absorption spectrum of an atom strongly coupled to a high-temperature reservoir

A. G. Kofman

Department of Chemical Physics, The Weizmann Institute of Science, Rehovot 76100, Israel

(Received 15 March 2004; published 9 March 2005)

We study the absorption spectrum of a weak probe field near resonant to an atomic transition, the upper level of which is strongly coupled to a third level by the interaction with a Lorentzian bosonic reservoir, such as, e.g., a mode of a high- $Q$  cavity or a local vibration in a solid. The reservoir coupling is approximated by the interaction with a classical complex Gaussian-Markovian random process (control field), which is justified when the reservoir temperature exceeds significantly the mode frequency or when the high- $Q$  cavity is pumped by broadband incoherent radiation. The present theory is applicable also when the control field is chaotic laser light. We assume that the rms control-field Rabi frequency  $V_0$  is much greater than the field detuning  $\Delta_c$ , which, in turn, is much greater than the material relaxation constants. We reveal and describe analytically all qualitatively different regimes of the spectrum modification and obtain their validity conditions. The analytical results are verified by numerical calculations using the exact continued-fraction solution. The analytical formulas obtained allow one to perform fast computer calculations for arbitrarily small values of the reservoir (control-field) bandwidth  $\nu$ , in contrast to the known numerical methods, which require sharply increasing computational resources with a decrease of  $\nu$ . In the most interesting case  $\nu \ll V_0$ , the spectrum consists of two peaks, the nonvanishing bandwidth and material relaxation affecting mainly the dip between the peaks. The results obtained in the static limit (i.e., a very narrow reservoir) are independent of the reservoir band shape. We reveal reservoir-induced transparency (RIT)—i.e., absorption reduction due to the reservoir coupling. Moreover, two unexpected, remarkable features are uncovered in a range of intermediate values of  $\nu$  and  $V_0$ ,  $\Gamma^2 |\Delta_c| \ll V_0^2 \nu \ll |\Delta_c|^3$  ( $\Gamma$  is the spectral width in the absence of the control field): an *extra peak* in the dip and a resonance-absorption *decrease* by a half (i.e., an *increase of RIT*) relative to the static limit. The existence of the above spectral features depends on the statistical details of the control-field temporal behavior.

DOI: 10.1103/PhysRevA.71.033806

PACS number(s): 42.50.Gy, 03.65.Yz, 42.50.Hz, 02.50.-r

## I. INTRODUCTION

Decoherence of quantum systems due to their interactions with the environment is the main obstacle for quantum computation and therefore it has attracted a significant interest in recent years [1]. The system-environment coupling is often weak, so that effects of the environment on quantum systems can be treated perturbatively or by such standard methods as master equations, cumulant expansions, quantum Monte Carlo simulations, etc. [2–4]. The strong-coupling case is much less understood. It was studied, e.g., for the familiar spin-boson model [5], where the system-reservoir interaction commutes with the (unperturbed) system Hamiltonian (a “diagonal” coupling).

An “off-diagonal” coupling of a quantum system to a reservoir, which is of interest here, may become strong, whenever there is a sharp feature in the reservoir (near) resonant to a quantum transition in the system [6]. The evolution of a two-level system coupled to a zero-temperature reservoir can be obtained exactly for the general case [6–8] and therefore is rather well understood. However, the finite-temperature case is much less amenable to an analytical solution and, therefore, remains still largely unexplored.

To be more specific, we consider a narrow bosonic reservoir with the Lorentzian spectral shape, such as, e.g., a damped quantum oscillator. This case is realized in a number of diverse physical situations, including, in particular, (a) impurities in solids interacting with local vibrations [9–11], (b) an atom coupled to a high- $Q$  optical [12] or microwave [13,14] cavity mode, (c) a nuclear spin attached to a nano-

mechanical oscillator (cantilever) [15], and (d) the electron spin of a magnetic impurity in a quantum-Hall-effect system interacting with localized phonons [16].

The population relaxation and resonance fluorescence spectrum of a two-level atom coupled to a thermal cavity mode was studied numerically in [17]. In a recent paper [18] the dynamics of a two-level system strongly coupled to a Lorentzian bosonic reservoir centered at the energy  $\hbar\omega_c$  was studied *analytically* in the limit of a high temperature  $T, k_B T \gg \hbar\omega_c$ , where  $k_B$  is the Boltzmann constant. Such a limit is obtained, e.g., when the ambient temperature is sufficiently high (which is achievable at microwave frequencies) or when a high- $Q$  cavity is pumped by broadband incoherent radiation (achievable at optical and microwave frequencies). A warm reservoir may have an advantage when a strong coupling is required, since the coupling intensity is proportional to  $T$  in the high-temperature limit. Moreover, the problem of an atom strongly coupled to a thermal reservoir (e.g., a damped cavity) is of principal importance in the quantum theory of damping [4]. Surprisingly, in Ref. [18] the decoherence was shown to occur *much slower* than the population relaxation [19], in sharp contrast to the familiar cases of a weak and/or zero-temperature coupling.

In the present paper, unlike [17,18], we assume that the reservoir couples *unpopulated* levels of an atom and study the modification of the absorption spectrum of a weak probe field at an adjacent transition. In terms of case (a), we consider the zero-photon line shape of an impurity coupled to a local vibration mode. Previously, this problem was studied for a weak coupling and arbitrary temperature, when the res-

ervoir was shown to induce the (temperature-dependent) broadening and shift of the line [9]. In contrast, a strong coupling can split the line into two peaks, as was shown for case (b), where the problem was solved for zero temperature and an arbitrary coupling strength. In particular, a strong atom-mode coupling causes such phenomena as the vacuum Rabi splitting [20], population trapping [21], and lasing without inversion [22,23].

In the high-temperature limit specified above, one can approximate the coupling to a bosonic reservoir by the interaction with a classical chaotic (complex Gaussian) field [18,19,24–26]. This allows one to use in the present case the results obtained for the absorption-spectrum modification by a chaotic field with a Lorentzian spectrum [27–33]. References [30–33] provided a comprehensive description of the absorption-spectrum modification by a (near)-resonant chaotic control field of an arbitrary intensity. In particular, it appeared that a strong field can split the spectrum into either two or even *three* peaks. Moreover, we revealed electromagnetically induced transparency (EIT) of the same order of magnitude as (or even equal to) EIT induced by a coherent monochromatic field [34,35]. With the increase of the field bandwidth, the EIT generally decreases, but sometimes [31,33] *can increase*. The case of an off-resonant chaotic field was treated previously only for a sufficiently weak coupling [29]. This case can be important practically, e.g., to avoid Doppler broadening [35]. A decrease of absorption due to a reservoir is called here the reservoir-induced transparency (RIT), by analogy with EIT. The phenomenon of RIT is equivalent to EIT in the situations, when the reservoir can be substituted by a laser field, such as, e.g., in the case of zero- [21,22] and high-temperature electromagnetic reservoirs.

In the present paper we consider an atom strongly and off resonantly coupled to a high-temperature Lorentzian bosonic reservoir. The absorption spectrum at an adjacent transition is studied, special attention being paid to the RIT. We focus on two important occurrences of the RIT: at the material resonance (RIT1) and at the absorption minimum (RIT2). We use several approximate analytical approaches, which allow us to reveal and describe all qualitatively different regimes of the probe-spectrum modification. An important advantage of the analytical formulas obtained is that they allow one to perform fast computer calculations for arbitrarily small values of the control-field (mode) bandwidth  $\nu$ . In contrast, computational resources required for the known numerical techniques, such as the Monte Carlo method [25], numerical solution of partial differential equations [31,32], and the continued-fraction calculation [32,33], sharply increase with a decrease of  $\nu$ .

The paper organization is as follows. The problem is formulated in Sec. II. Section III is devoted to the static limit, where the reservoir (field) spectral width  $\nu$  is very small. Now the spectrum consists of two broad peaks, material relaxation affecting mainly the dip between them. The results of Sec. III hold *irrespective of the reservoir spectral shape*. The case of a Lorentzian reservoir with an arbitrary width is studied analytically and numerically in Secs. IV (the formalism) and V (the absorption spectrum). In particular, it appears that in a certain interval of the rms coupling amplitudes  $V_0$  (or  $\nu$ ) RIT2 is independent of  $V_0$ . Moreover, two unex-

pected, remarkable spectral features are revealed for intermediate values of  $V_0$  (or  $\nu$ ): an *extra peak* in the dip and a resonance-absorption coefficient *decrease* by a half relative to the static limit. Section VI provides concluding remarks. The Appendix contains details of the derivations.

## II. FORMULATION OF THE PROBLEM

Consider a medium consisting of three-level atoms with the ground state  $|g\rangle$  and two other states  $|a\rangle$  and  $|b\rangle$ . The atoms are assumed to be homogeneously broadened, the half width at half maximum of transitions  $|g\rangle-|a\rangle$  and  $|g\rangle-|b\rangle$  being  $\Gamma$  and  $\Gamma'$ , respectively. If the transition  $|a\rangle-|b\rangle$  is linearly coupled to a narrow high-temperature bosonic reservoir, the atomic Hamiltonian in the rotating-wave approximation is [18]

$$H(t) = -\hbar\Delta_c|b\rangle\langle b| + \hbar[V_c(t)|b\rangle\langle a| + \text{H.c.}]. \quad (2.1)$$

Here the coupling amplitude  $V_c(t)$  is a complex Gaussian process and the reservoir (field) detuning  $\Delta_c = \omega_c - \omega_{ba}$ , where  $\omega_c$  is the center frequency of the reservoir (field),  $\omega_{ij} = \omega_i - \omega_j$ , and  $\hbar\omega_i$  is the energy of level  $|i\rangle$ . The Hamiltonian (2.1) describes also the coupling to a chaotic electromagnetic field [30]:

$$\mathcal{E}_c(t) = E_c(t)e^{-i\omega_c t} + \text{c.c.} \quad (2.2)$$

Then the coupling amplitude  $V_c(t) = -d_{ba}E_c(t)/\hbar$  is called the (complex) Rabi frequency,  $d_{ij}$  being the dipole matrix element for transition  $|i\rangle-|j\rangle$ .

The reservoir [or the control field  $\mathcal{E}_c(t)$ ] modifies absorption of a weak probe field near resonant to the dipole-allowed transition  $|g\rangle-|a\rangle$  ( $|a\rangle$  and  $|b\rangle$  are assumed to be empty in the absence of the probe field). The probe-field absorption coefficient  $\bar{\alpha}(\omega)$  is [31]

$$\bar{\alpha}(\omega) = \frac{4\pi N\omega|d_{ag}|^2}{\hbar c} \bar{A}(\Delta), \quad (2.3)$$

where  $\bar{A}(\Delta)$  is the scaled absorption coefficient,  $c$  is the vacuum speed of light,  $\omega$  is the probe-field frequency,  $N$  is the number of the atoms per unit volume, and  $\Delta = \omega - \omega_{ag}$  is the probe-field detuning. The absorption coefficient is averaged over the field fluctuations, which is denoted by the overbar in Eq. (2.3).

The reservoir can produce a decrease of the probe absorption at certain frequencies (reservoir-induced transparency), which is compensated by an increase of the probe absorption at other frequencies, in view of the sum rule [32,36]

$$\int_{-\infty}^{\infty} \bar{A}(\Delta) d\Delta = \pi. \quad (2.4)$$

Below we often call  $V_c(t)$  the Rabi frequency and use the term “control field” instead of “reservoir” to be in line with previous papers [30–33]. We assume, for definiteness, the ladder scheme ( $\omega_g < \omega_a < \omega_b$ ); however, all the subsequent results remain valid also for the  $\Lambda$  scheme ( $\omega_b > \omega_a, \omega_g$ ) upon the substitution [30]

$$\omega_c \rightarrow -\omega_c. \quad (2.5)$$

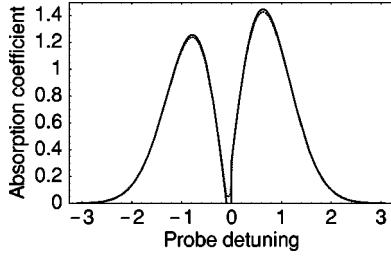


FIG. 1. The static line shape  $\bar{A}_{st}(\Delta)$  for  $V_0=1$  and  $\Delta_c=0.1$  with  $\Gamma=\Gamma'=0$  (solid curve) and  $\Gamma=\Gamma'=0.01$  (dotted curve).

Taking into account that the average Rabi frequency  $\bar{V}_c(t)=0$ , the reservoir (control field) is characterized by the rms Rabi frequency  $V_0=(|V_c|^2)^{1/2}$ , the bandwidth  $\nu$ , and the detuning  $\Delta_c$ . In the present paper we focus on the situation of a strong, off-resonant control field, when the detuning dominates the material relaxation constants, but is less than  $V_0$ :

$$(a) V_0 \gg |\Delta_c|, \quad (b) |\Delta_c| \gg \Gamma, \Gamma'. \quad (2.6)$$

Below we mainly concentrate on the strong-coupling case

$$V_0 \gg \nu. \quad (2.7)$$

Under conditions (2.6) and (2.7) the spectrum is approximately symmetric, being split into two peaks (Autler-Towns splitting [37]). Then the main effect of the material relaxation and the field bandwidth is to modify the line shape of the dip between the peaks, as shown below.

### III. STATIC LIMIT (VERY NARROW RESERVOIR)

Here we consider the limit where the reservoir (control-field) bandwidth  $\nu$  is negligibly small (quasistatic regime). In this case, the coupling amplitude  $V_c(t)$  is changing very slowly and the spectrum can be obtained by averaging that for a coherent control field over the Rayleigh distribution

$$f(V) = (2V/V_0^2) \exp(-V^2/V_0^2), \quad (3.1)$$

with  $V=|V_c|$ , yielding [30]

$$\bar{A}_{st}(\Delta) = V_0^{-2} \text{Re} \tilde{\Gamma}' e^{\tilde{\Gamma}'/V_0^2} E_1(\tilde{\Gamma}'/V_0^2). \quad (3.2)$$

Here  $E_1(\dots)$  is an integral exponential function [38] and

$$\tilde{\Gamma} = \Gamma - i\Delta, \quad \tilde{\Gamma}' = \Gamma' - i\Delta', \quad (3.3)$$

where

$$\Delta' = \Delta + \Delta_c = \omega + \omega_c - \omega_{bg} \quad (3.4)$$

is the two-photon detuning. Note that Eq. (3.2) and the subsequent results of this section are independent of the band shape of the reservoir (or the control field).

For sufficiently small detunings  $\Delta$ , so that  $V_0^2 \gg (\Gamma + |\Delta|) \times (\Gamma' + |\Delta'|)$  or, in view of Eq. (2.6),

$$|\Delta| \ll V_0, \quad (3.5)$$

Eq. (3.2) yields in the first approximation [30,31]

$$\begin{aligned} \bar{A}_{st}(\Delta) = \frac{1}{V_0^2} & \left[ \Gamma' \ln \frac{C_1 V_0^2}{\sqrt{(\Gamma^2 + \Delta^2)(\Gamma'^2 + \Delta'^2)}} \right. \\ & \left. + \Delta' \left( \arctan \frac{\Delta}{\Gamma} + \arctan \frac{\Delta'}{\Gamma'} \right) \right]. \quad (3.6) \end{aligned}$$

Here  $C_1 = e^{-\gamma} \approx 0.56$ , where  $\gamma \approx 0.58$  is the Euler constant [38].

### A. Spectral shape

#### 1. Vanishing relaxation

In the limit of the vanishing material relaxation,

$$\Gamma, \Gamma' \rightarrow 0, \quad (3.7)$$

Eq. (3.2) becomes [39] (see the solid line in Fig. 1)

$$\bar{A}_{st}(\Delta) = \frac{\pi |\Delta'|}{V_0^2} e^{-\Delta \Delta' / V_0^2} \theta(\Delta \Delta'). \quad (3.8)$$

Equation (3.8) implies that there is a complete transparency

$$\bar{A}_{st}(\Delta) = 0 \quad \text{for } \Delta \Delta' < 0, \quad (3.9)$$

i.e., for  $\Delta$  in the interval between one- and two-photon resonances (0 and  $-\Delta_c$ , respectively), whereas at the frequencies of the one- and two-photon resonances there are discontinuities of the spectrum and its derivative, respectively.

Outside of a narrow central part, the spectrum (3.8) can be approximated [due to Eq. (2.6)] as

$$\bar{A}_{st}(\Delta) \approx \frac{\pi}{2} \left( 1 + \frac{\Delta_c}{2\Delta} \right) f \left( \left| \Delta + \frac{\Delta_c}{2} \right| \right) \quad (|\Delta| \gg |\Delta_c|). \quad (3.10)$$

Equation (3.10) shows that the spectrum is nearly mirror symmetric with respect to  $\Delta = -\Delta_c/2$ . The asymmetry of the spectrum arises from the factor in the parentheses in Eq. (3.10), which is close to 1 for  $|\Delta| \gg |\Delta_c|$ . The spectrum consists of two peaks with the maxima

$$\bar{A}_{st}(\pm \Delta_m) \approx (\pi/\sqrt{2}e) V_0^{-1}, \quad \Delta_m \approx V_0/\sqrt{2}; \quad (3.11)$$

the peaks approximately mimic the amplitude distribution (3.1) and have width on the order of  $V_0$ .

The spectrum (3.8) can be interpreted as the Autler-Towns doublet induced by a coherent control field, which is inhomogeneously broadened due to the distribution (3.1) [40]. The small- and large-detuning cases discussed above correspond to the weak- ( $V \lesssim |\Delta_c|$ ) and strong- ( $V \gg |\Delta_c|$ ) field cases of the Autler-Towns splitting.

#### 2. Nonvanishing relaxation

The effects of nonvanishing material relaxation show up at frequencies, where the absorption is weak—i.e., in the dip between the peaks and at the wings of the spectrum (see Fig. 1). The transformation of the dip is of the main interest. In view of the smallness of the relaxation constants with respect to the detuning [Eq. (2.6)], the dip can be considered as consisting of three overlapping parts: the two edges of the

dip in the vicinities of the one- and two-photon resonances and the bottom of the dip, as follows.

When  $\Gamma$  ( $\Gamma'$ ) is nonzero, the above spectral sharp feature at  $\Delta=0$  ( $\Delta=-\Delta_c$ ) is smoothed out. Indeed, as follows from Eq. (3.6), for  $|\Delta| \ll |\Delta_c|$  on the outer side of the one-photon frequency (i.e., the side farther from the two-photon frequency), where  $\Delta_c \Delta > 0$ , and for  $|\Delta| \leq \Gamma$  on the inner side ( $\Delta_c \Delta < 0$ ),

$$\bar{A}_{st}(\Delta) = \frac{1}{V_0^2} \left( \frac{\pi}{2} |\Delta'| + \Delta' \arctan \frac{\Delta}{\Gamma} \right). \quad (3.12)$$

Equation (3.12) simplifies, for sufficiently large detunings on the outer side,

$$\bar{A}_{st}(\Delta) \approx \frac{\pi |\Delta'|}{V_0^2} - \frac{\Gamma \Delta_c}{V_0^2 \Delta} \quad (\Gamma \ll |\Delta| \ll |\Delta_c|), \quad (3.13)$$

this expression being close to Eq. (3.8).

Similarly, for  $|\Delta'| \ll |\Delta_c|$  on the outer side of the two-photon resonance ( $\Delta_c \Delta' < 0$ ) and for  $|\Delta'| \leq \Gamma'$  on the inner side ( $\Delta_c \Delta' > 0$ ), Eq. (3.6) yields

$$\bar{A}_{st}(\Delta) = \frac{1}{V_0^2} \left( \Delta' \arctan \frac{\Delta'}{\Gamma'} - \frac{\pi \Delta'}{2} \operatorname{sgn} \Delta_c + \Gamma' \ln \frac{C_1 V_0^2}{|\Delta_c| \sqrt{\Gamma'^2 + \Delta'^2}} \right), \quad (3.14)$$

where  $\operatorname{sgn} \Delta_c = \Delta_c / |\Delta_c|$ . Expression (3.14) is a monotonous function, which becomes, on the outer side for  $\Gamma' \ll |\Delta'| \ll |\Delta_c|$ ,

$$\bar{A}_{st}(\Delta) \approx \pi |\Delta'| / V_0^2, \quad (3.15)$$

overlapping with Eq. (3.8).

The frequency interval between the one- and two-photon resonances, defined by  $\Delta \Delta' < 0$  with  $|\Delta| \geq \Gamma$  and  $|\Delta'| \geq \Gamma'$ , is a low-absorption region (the bottom of the dip). In the above interval Eq. (3.6) yields

$$\bar{A}_{st}(\Delta) = \frac{1}{V_0^2} \left( \frac{\Gamma |\Delta'|}{|\Delta|} + \Gamma' \ln \frac{C_2 V_0^2}{|\Delta \Delta'|} \right), \quad (3.16)$$

where  $C_2 = e^{-\gamma-1} \approx 0.21$ . Equation (3.16) describes an asymmetric dip.

Finally, the far wings of the spectrum follow from Eq. (3.2) on using the asymptotic formula for the integral exponential function [38],

$$\bar{A}_{st}(\Delta) = \frac{\Gamma}{\Delta^2} + \frac{V_0^2 \Gamma'}{\Delta^4} \quad (|\Delta| \gg V_0). \quad (3.17)$$

The second term here can be appreciable for  $\Gamma' \gg \Gamma$ .

### B. RIT

As mentioned above, the control field decreases and increases absorption in different spectral intervals. In the present off-resonant case there are two frequencies, where a decrease of absorption is especially important. First, RIT always occurs at the resonance frequency (RIT1), since the

control field generally broadens and shifts (and possibly splits) the spectral line. For the present case in the static limit, RIT1 is given by [see Eq. (3.12)]

$$\bar{A}_{st}(0) = \frac{\pi |\Delta_c|}{2V_0^2}. \quad (3.18)$$

Second, there is a possibility of RIT (called here RIT2) at the absorption minimum between the one- and two-photon resonances. From Eq. (3.16) we obtain the absorption-minimum position and value, respectively, to be

$$\Delta_m = - \frac{1 - G + \sqrt{1 + 6G + G^2}}{4} \Delta_c \equiv -q(G) \Delta_c, \quad (3.19)$$

$$\bar{A}_{st}(\Delta_m) = \frac{\Gamma'}{V_0^2} \ln \frac{KV_0^2(\Gamma + \Gamma')}{\Gamma' \Delta_c^2}. \quad (3.20)$$

Here  $G = \Gamma/\Gamma'$  and the quantity

$$K = \frac{C_1 e^{G/q(G)-G-1}}{(1+G)q(G)[1-q(G)]} \quad (3.21)$$

[with  $q(G)$  defined in (3.19)] weakly depends on  $G = \Gamma/\Gamma'$ , varying from  $C_1$  for  $\Gamma' \ll \Gamma$  to  $(4/e)C_1 \approx 1.47C_1$  for  $\Gamma' \gg \Gamma$ .

For  $\Gamma' \ll \Gamma$ , Eq. (3.19) implies that the minimum of absorption (RIT2) is achieved near the two-photon resonance, viz., at

$$\Delta = \Delta_m = -(1 - \Gamma'/\Gamma) \Delta_c, \quad (3.22)$$

whereas the value at the minimum follows from Eq. (3.20):

$$\bar{A}_{st}(\Delta_m) = \frac{\Gamma'}{V_0^2} \ln \frac{C_1 V_0^2 \Gamma}{\Gamma' \Delta_c^2} \quad (\Gamma' \ll \Gamma). \quad (3.23)$$

In the opposite case  $\Gamma \ll \Gamma'$ , Eqs. (3.19)–(3.21) yield

$$\bar{A}_{st}(\Delta_m) = \frac{2\Gamma'}{V_0^2} \ln \frac{C_4 V_0}{|\Delta_c|}, \quad \Delta_m = -\Delta_c/2, \quad (3.24)$$

where  $C_4 = 2e^{-\gamma/2-1/2} \approx 0.91$ .

The fact that the minimal absorption coefficient (3.20) is proportional to  $\Gamma'$  is a result of quantum interference, which is destructive for  $\Gamma' < \Gamma$  and constructive for  $\Gamma' > \Gamma$  [30,35]. For strong destructive interference  $\Gamma' \ll \Gamma$ , the position of the absorption minimum (3.22) is close to the two-photon resonance. In the case  $\Gamma' = 0$ , the probe absorption vanishes at the exact two-photon resonance  $\Delta' = 0$  (or  $\Delta = -\Delta_c$ ). With the increase of  $\Gamma'$  the position of the minimum moves towards the one-photon resonance, reaching the middle point between the one- and two-photon resonances in the case of strong constructive interference  $\Gamma' \gg \Gamma$  [see Eq. (3.24)].

In the case of the coherent control field the absorption minimum is obtained at  $\Delta_m = -\Delta_c(\Gamma + \Gamma')/(\Gamma + 2\Gamma')$  [30]. This dependence of  $\Delta_m$  on  $\Gamma$  and  $\Gamma'$  is very similar to that in Eq. (3.19). In the case of the coherent control field the absorption minimum  $A(\Delta_m) = \Gamma'/V_0^2$  [30]. Comparing the latter result with Eq. (3.20) shows that an off-resonant intensity-fluctuating control field creates RIT2 of the same order of

magnitude as that due to a coherent field of the same intensity. This conclusion extends the similar observation made earlier [30] for the (near-)resonant case.

Note that for the absorption minimum to be interpreted as RIT2, the inequality

$$\bar{A}(\Delta_m) \ll A_0(\Delta_m) \quad (3.25)$$

should hold, where

$$A_0(\Delta) = \Gamma/(\Gamma^2 + \Delta^2) \quad (3.26)$$

is the absorption coefficient in the absence of the control field. As follows from Eqs. (3.19) and (3.20), in the off-resonance case (2.6) the inequality (3.25) is equivalent to

$$V_0^2 \gg \Gamma' \Delta_c^2 \Gamma. \quad (3.27)$$

Inequality (3.27) is violated only for very strong constructive interference—viz., for  $\Gamma'/\Gamma \gg V_0^2/\Delta_c^2 \gg 1$  [cf. Eq. (2.6)]. We should mention that the RIT2 condition (3.27), obtained here for an intensity-fluctuating field with the distribution (3.1), coincides with that for a coherent field [30].

#### IV. CHAOTIC FIELD

##### A. Formalism

In Sec. III we have considered the limit of a very-narrow-band reservoir (control field) with an arbitrary spectral shape. To take into account effects of a final bandwidth, we consider a Lorentzian band shape

$$g_c(\omega) = \frac{V_0^2 \nu}{\pi(\omega^2 + \nu^2)}. \quad (4.1)$$

As mentioned in Sec. II,  $V_c(t)$  is a complex Gaussian process, called also a chaotic field [24,25]. Its correlation function, given by the Fourier transform Eq. (4.1), is exponential,  $\langle V_c(t) V_c^*(0) \rangle = V_0^2 e^{-\nu t}$ ; hence,  $V_c(t)$  is both Gaussian and Markovian.

Now the probe absorption spectrum is given by [30]

$$\bar{A}(\Delta) = 2\pi \operatorname{Re} \left( \int_0^\infty \Psi_a(V) V dV \right). \quad (4.2)$$

Here  $\Psi_a(V)$  and an auxiliary quantity  $\tilde{\Psi}_b(V)$  obey the equations [30,32]

$$-\tilde{\Gamma} \Psi_a - V \tilde{\Psi}_b + L_0 \Psi_a = -f(V), \quad (4.3a)$$

$$-\tilde{\Gamma}' \tilde{\Psi}_b + V \Psi_a + L_1 \tilde{\Psi}_b = 0, \quad (4.3b)$$

where the stochastic operators [18]

$$L_0 = \frac{\nu}{V} \frac{\partial}{\partial V} V^2 + \frac{V_0^2 \nu}{2V} \frac{\partial}{\partial V} \left( V \frac{\partial}{\partial V} \right), \quad L_1 = L_0 - \frac{V_0^2 \nu}{2V^2}. \quad (4.4)$$

The first term in  $L_0$  is similar to that arising in a diffusion equation due to an external force, whereas the other terms in  $L_0$  and  $L_1$  correspond to a free diffusion (in the absence of an external force) in the  $V_c$  plane with the diffusion coefficient  $D = V_0^2 \nu / 2$ .

There exists no exact closed solution of Eqs. (4.3). Therefore we shall employ three approximate analytical solutions valid in different, but overlapping, regions. Two of these solutions were obtained previously [30,31,33], but were not yet analyzed for the strong, off-resonant coupling. The analytical results are verified in Sec. V by numerical calculations performed with the help of the exact solution in the form of a continued fraction [33].

##### B. Previously known analytical solutions

###### 1. Neglect of $L_1 \tilde{\Psi}_b$

If  $|\Delta'|$  is sufficiently large, the third term on the left-hand side of Eq. (4.3b) is small in comparison with the first term and can be neglected in the first approximation. Then the solution of Eqs. (4.3) is [31,33]

$$\bar{A}(\Delta) = \operatorname{Re} \left( \frac{F(1, 1; 1 + d_0; -z_0)}{\Gamma - i\Delta + (\beta_0 - 1)\nu} \right), \quad (4.5)$$

where  $F(\dots)$  is the hypergeometric function [38] and

$$\beta_0 = \left( 1 + \frac{2V_0^2}{\nu \tilde{\Gamma}'} \right)^{1/2}, \quad d_0 = \frac{\tilde{\Gamma} + (\beta_0 - 1)\nu}{2\beta_0 \nu},$$

$$z_0 = \frac{(\beta_0 - 1)^2}{4\beta_0}. \quad (4.6)$$

As shown in the Appendix, sufficient conditions for the validity of Eq. (4.5) are

$$(V_0^2 \nu)^{1/2} \ll |\Delta_c|^{3/2} \quad (4.7)$$

and

$$|\Delta| \ll |\Delta_c|. \quad (4.8)$$

Consider the special cases of Eq. (4.5). In the limit  $\nu \rightarrow 0$ , Eq. (4.5) can be shown to reduce to the exact static-limit result (3.2). For the strong-field case in study, Eq. (2.6), the dip region, Eq. (3.5), can be described by the simplified expression [31,33]

$$\bar{A}(\Delta) = \operatorname{Re} \left\{ \frac{\tilde{\Gamma}'}{V_0^2} \left[ \frac{1}{2} \ln \frac{C_1^2 V_0^2}{8\nu \tilde{\Gamma}'} - \psi \left( a_0 + \frac{1}{2} \right) \right] \right\}. \quad (4.9)$$

Here  $\psi(\dots)$  is the logarithmic derivative of the  $\Gamma$  function [38] and  $a_0 = \tilde{\Gamma} [\tilde{\Gamma}' / (8V_0^2 \nu)]^{1/2}$ .

###### 2. Neglect of $L_0 \Psi_a$

Similarly to the above, if  $|\Delta|$  is sufficiently large, the third term on the left-hand side of Eq. (4.3a) can be neglected in the first approximation. This yields the analytical solution [30]

$$\bar{A}(\Delta) = \frac{\Gamma}{\Gamma^2 + \Delta^2} - V_0^2 \operatorname{Re} \left( \frac{F(1, 2; 1 + d; -z)}{\tilde{\Gamma}^2 [\tilde{\Gamma}' + (2\beta - 1)\nu]} \right), \quad (4.10)$$

where

$$\beta = \sqrt{1 + 2V_0^2/(\nu\tilde{\Gamma})}, \quad z = (\beta - 1)^2/(4\beta),$$

$$d = [(2\beta - 1)\nu + \tilde{\Gamma}']/(2\beta\nu). \quad (4.11)$$

As shown in the Appendix, sufficient conditions for the validity of Eq. (4.10) are Eq. (4.7) and

$$|\Delta'| \ll |\Delta_c|. \quad (4.12)$$

Consider special cases. In the limit  $\nu \rightarrow 0$ , Eq. (4.10) tends to the static result (3.2) [30]. In the case (2.6) and (3.5), Eq. (4.10) can be reduced in the first approximation to [30]

$$\bar{A}(\Delta) = \text{Re} \left\{ \frac{\tilde{\Gamma}'}{V_0^2} \left[ \frac{1}{2} \ln \frac{C_1^2 V_0^2}{8\nu\tilde{\Gamma}} - \psi(a+1) + \frac{1}{2a} \right] \right\}, \quad (4.13)$$

where  $a = \tilde{\Gamma}'[\tilde{\Gamma}/(8V_0^2\nu)]^{1/2}$ .

### C. Small- $\nu$ corrections

The above approximate solutions were obtained by neglecting one of the two stochastic terms in Eqs. (4.3). An alternative analytical approach is to consider corrections to the static solution.

If both  $|\tilde{\Gamma}|$  and  $|\tilde{\Gamma}'|$  are sufficiently large, the stochastic terms in Eqs. (4.3) can be taken into account perturbatively. To this end, we cast Eq. (4.3) in a matrix form

$$B\Psi(V) = F + M\Psi(V), \quad (4.14)$$

where  $\Psi = (\Psi_a, \Psi_b)^T$  and  $F = (f(V), 0)^T$  are column vectors and

$$B = \begin{pmatrix} \tilde{\Gamma} & V \\ -V & \tilde{\Gamma}' \end{pmatrix}, \quad M = \begin{pmatrix} L_0 & 0 \\ 0 & L_1 \end{pmatrix}. \quad (4.15)$$

In the zero approximation we neglect  $M\Psi$  in Eq. (4.14) and obtain

$$\Psi(V) \approx \Psi^{\text{st}}(V) = B^{-1}F, \quad (4.16)$$

where  $\Psi^{\text{st}}(V)$  is the solution of Eqs. (4.3) in the static limit ( $\nu \rightarrow 0$ ) and

$$B^{-1} = \frac{1}{V^2 + \tilde{\Gamma}\tilde{\Gamma}'} \begin{pmatrix} \tilde{\Gamma}' & -V \\ V & \tilde{\Gamma} \end{pmatrix}. \quad (4.17)$$

In the next approximation, we insert

$$\Psi(V) = \Psi^{\text{st}}(V) + \Psi^{(1)}(V) \quad (4.18)$$

into Eq. (4.14) and set  $M\Psi(V) \approx M\Psi^{\text{st}}(V)$ , yielding

$$\Psi^{(1)}(V) = B^{-1}M\Psi^{\text{st}}(V). \quad (4.19)$$

Thus,

$$\Psi_a(V) = \Psi_a^{\text{st}}(V) + \Psi_a^{(1)}(V), \quad (4.20)$$

where

$$\Psi_a^{\text{st}}(V) = \tilde{\Gamma}'f(V)/(V^2 + \tilde{\Gamma}\tilde{\Gamma}'), \quad (4.21)$$

$$\Psi_a^{(1)}(V) = \frac{1}{V^2 + \tilde{\Gamma}\tilde{\Gamma}'} \left[ L_0 \frac{\tilde{\Gamma}'^2 f(V)}{V^2 + \tilde{\Gamma}\tilde{\Gamma}'} - VL_1 \frac{Vf(V)}{V^2 + \tilde{\Gamma}\tilde{\Gamma}'} \right]. \quad (4.22)$$

Inserting Eq. (4.20) into Eq. (4.2) on account of Eqs. (4.22) and (4.4) and integrating by parts yields

$$\bar{A}(\Delta) = \bar{A}_{\text{st}}(\Delta) + \bar{A}_d(\Delta) + \bar{A}_f(\Delta), \quad (4.23)$$

where  $\bar{A}_d(\Delta)$  and  $\bar{A}_f(\Delta)$  correspond to the free-diffusion and force terms in  $L_0$  and  $L_1$  [see the remark after Eq. (4.4)]:

$$\bar{A}_d(\Delta) = 2\nu \text{Re} \left\{ \frac{e^b}{\tilde{\Gamma}\tilde{\Gamma}'} \left[ \left( \frac{\tilde{\Gamma}'}{\tilde{\Gamma}} + 2 \right) E_3(b) - 2 \left( \frac{\tilde{\Gamma}'}{\tilde{\Gamma}} + 1 \right) E_4(b) \right] \right\}, \quad (4.24a)$$

$$\bar{A}_f(\Delta) = \nu V_0^{-2} \text{Re} \left\{ e^b \{ 2\tilde{\Gamma}'\tilde{\Gamma}^{-1} [E_2(b) - E_3(b)] - E_1(b) + 3E_2(b) - 2E_3(b) \} \right\}. \quad (4.24b)$$

Here  $b = \tilde{\Gamma}\tilde{\Gamma}'/V_0^2$  and  $E_n(b) = \int_1^\infty x^{-n} e^{-bx} dx$  is an integral exponential function [38]. In the derivation of Eqs. (4.24) we used the equality

$$\int_0^\infty (x+b)^{-n} e^{-x} dx = b^{1-n} e^b E_n(b). \quad (4.25)$$

It can be shown [38] that, for  $|b| \ll 1$ ,

$$E_1(b) \approx -\ln b - \gamma, \quad E_n(b) \approx (n-1)^{-1} (n > 1), \quad (4.26a)$$

whereas, for  $|b| \gg 1$ ,

$$E_n(b) = b^{-1} e^{-b} [1 - n/b + O(|b|^{-2})]. \quad (4.26b)$$

It is useful to note that the summands proportional to  $\tilde{\Gamma}'$  in the brackets of Eq. (4.24a) and in the braces of Eq. (4.24b) result from the term  $L_0\Psi_a$  in Eqs. (4.3), the other summands resulting, correspondingly, from the term  $L_1\Psi_b$  in Eqs. (4.3) [cf. Eq. (4.22)].

In the dip region (3.5), in view of Eq. (2.6), one obtains

$$V_0 \gg |\tilde{\Gamma}|, |\tilde{\Gamma}'|. \quad (4.27)$$

In this case  $|b| \ll 1$  and one obtains from Eqs. (4.24) and (4.26a) that

$$\bar{A}_d(\Delta) \approx \text{Re} \left[ \frac{\nu}{3\tilde{\Gamma}} \left( \frac{2}{\tilde{\Gamma}'} - \frac{1}{\tilde{\Gamma}} \right) \right], \quad (4.28a)$$

$$\bar{A}_f(\Delta) \approx \frac{\nu}{V_0^2} \text{Re} \left[ \frac{\tilde{\Gamma}'}{\tilde{\Gamma}} + \ln \frac{\tilde{\Gamma}\tilde{\Gamma}'}{V_0^2} + 2 + \gamma \right]. \quad (4.28b)$$

In view of Eqs. (4.27) and (4.28),

$$\bar{A}_d(\Delta) \gg \bar{A}_f(\Delta) \quad (|\Delta| \ll V_0) \quad (4.29)$$

and hence  $\bar{A}_f(\Delta)$  can be neglected in Eq. (4.23), yielding

$$\bar{A}(\Delta) \approx \bar{A}_{st}(\Delta) + \bar{A}_d(\Delta). \quad (4.30)$$

## V. PROBE ABSORPTION SPECTRUM

In the case (2.7), which is of the main interest here, the reservoir width  $\nu$  is so narrow that the probe absorption spectrum is still close to the static limit. Modifications of the spectrum due to temporal fluctuations occur only in the frequency intervals where absorption is small—i.e., for the dip and spectral wings.

### A. Narrow-band field

For a narrow-band field, Eq. (4.7), a modification of the dip line shape due to a finite bandwidth  $\nu$  occurs in a frequency range, which includes the interval between the one- and two-photon resonances (defined by  $\Delta\Delta' < 0$ ) and close vicinities of the latter (4.8) and (4.12), whereas the main part of the static spectrum (3.8) remains unchanged.

#### 1. Dip shape

It is convenient to divide the dip into three overlapping parts, described by simple expressions (cf. Sec. III). In particular, in the intervals (4.8) and (4.12) the solutions (4.5) and (4.10), respectively, simplify to Eqs. (4.9) and (4.13). They describe smoothing of the edges of the two spectral components, which increases with the increase of  $\nu$ .

One can use the asymptotic expansion [38] of  $\psi(\dots)$  to obtain the formulas [31]

$$\psi(a_0 + 1/2) = \ln a_0 + (24a_0^2)^{-1} + O(|a_0|^{-4}) \quad (5.1a)$$

and [30]

$$\psi(a + 1) = \ln a + (2a)^{-1} - (12a^2)^{-1} + O(|a|^{-4}), \quad (5.1b)$$

which allow one to reduce the solutions (4.9) and (4.13) in the first approximation to the static limit (3.6). The validity conditions of the static limit in the intervals (4.8) and (4.12) are given by the inequalities  $|a_0|^2 \gg 1$  and  $|a|^2 \gg 1$ , respectively. The above inequalities are most restrictive for the one- and two-photon resonances, respectively, yielding the conditions

$$V_0^2 \nu \ll \Gamma^2 |\Delta_c|, \quad (5.2a)$$

$$V_0^2 \nu \ll \Gamma'^2 |\Delta_c|, \quad (5.2b)$$

respectively. When any of the conditions (5.2) is violated, the probe absorption significantly depends on  $\nu$ . As a result, the sharp features in vicinities of  $\Delta=0$  and  $\Delta=-\Delta_c$  become smoother.

Consider first the vicinity (4.8) of the one-photon resonance, where, under the condition

$$4\sqrt{V_0^2 \nu} \gg \Gamma\sqrt{|\Delta_c|} \quad (5.3)$$

opposite to Eq. (5.2a), the material constants can be dropped in Eq. (4.9) in the first approximation, yielding

$$\bar{A}(\Delta) \approx \frac{|\Delta'|}{V_0^2} \left\{ \frac{\pi}{4} - \text{Im} \psi \left( \frac{1}{2} - e^{\pi i/4} \frac{\Delta}{\sqrt{8l}} \right) \right\}. \quad (5.4)$$

Here  $l = \sqrt{V_0^2 \nu / |\Delta_c|} \text{sgn} \Delta_c$ ,  $|l| (\ll |\Delta_c|)$  being a characteristic length of change of the line shape (5.4). In view of Eq. (5.1a), the line shape (5.4) simplifies for sufficiently large detunings, yielding on the outer and inner sides of the one-photon resonance, respectively,

$$\bar{A}(\Delta) \approx \frac{\pi|\Delta'|}{V_0^2} + \frac{\nu}{3\Delta^2} \quad \left( \frac{\Delta}{l} \gg 1 \right), \quad (5.5a)$$

$$\bar{A}(\Delta) \approx \frac{\nu}{3\Delta^2} \quad \left( -\frac{\Delta}{l} \gg 1 \right). \quad (5.5b)$$

The most striking feature of the line shape (5.4) is the presence of a *bump* (*extra peak*). Numerical calculations yield the maximum

$$\bar{A}(\Delta_1) \approx \frac{1.17\pi|\Delta_c + \Delta_1|}{V_0^2}, \quad \Delta_1 \approx 1.53l. \quad (5.6)$$

Correspondingly, there is also a minimum, the position of which is obtained from Eq. (5.5a):  $\Delta_2 = (2V_0^2 \nu / 3\pi)^{1/3} \text{sgn} \Delta_c$ . This result holds for  $\Gamma \ll (V_0^2 \nu)^{2/3} / |\Delta_c|$ , whereas for  $(V_0^2 \nu)^{2/3} / |\Delta_c| \ll \Gamma \ll 4\sqrt{V_0^2 \nu / |\Delta_c|}$  the correction  $-\Gamma\Delta_c / V_0^2 \Delta$  should be included into Eq. (5.5a) [cf. Eq. (3.13)], yielding  $\Delta_2 = 2V_0^2 \nu / \Gamma\Delta_c$ .

The absorption at the one-photon resonance (RIT1) follows from Eq. (5.4) to be

$$\bar{A}(0) \approx \frac{\pi|\Delta_c|}{4V_0^2}. \quad (5.7)$$

In the present case, RIT1 has a remarkable feature. As follows from a comparison of Eqs. (3.18) and (5.7),  $\bar{A}(0) \approx \bar{A}_{st}(0)/2$ ; i.e., for a sufficiently large  $\nu$ , the absorption coefficient at the one-photon resonance (RIT1) is *approximately half* that in the static limit. Such a behavior is rather unusual, since in most cases, in agreement with intuition, transparency decreases with an increase of the rate of fluctuations  $\nu$  (a known exception is the constructive-interference case with a *resonant* control field [31,33]).

In a vicinity of the two-photon resonance (4.12) for

$$2\sqrt{V_0^2 \nu} \gg \Gamma'\sqrt{|\Delta_c|}, \quad (5.8)$$

terms involving  $\Gamma$  and  $\Gamma'$  can be neglected in Eq. (4.13) and we obtain

$$\bar{A}(\Delta) \approx \sqrt{\frac{\nu}{V_0^2 |\Delta_c|}} \left( 1 - \frac{\Delta'}{l} \left\{ \frac{\pi}{4} + \text{Im} \psi \left( 1 - e^{3\pi i/4} \frac{\Delta'}{\sqrt{8l}} \right) \right\} \right). \quad (5.9)$$

As follows from this equation,

$$\bar{A}(\Delta) \approx \sqrt{\frac{\nu}{V_0^2 |\Delta_c|}} \quad (|\Delta'| \ll \sqrt{V_0^2 \nu / |\Delta_c|}); \quad (5.10)$$

i.e., the absorption at the two-photon resonance  $\Delta'=0$  increases with  $\nu$ . On the outer side of the two-photon reso-

nance ( $\Delta_c \Delta' < 0$ ) for  $|\Delta'| \gg \sqrt{V_0^2 \nu / |\Delta_c|}$  the quasistatic line shape [Eq. (3.8)] remains practically unchanged. This results from the fact that Eq. (5.9) reduces to Eq. (3.15) for  $\sqrt{V_0^2 \nu / |\Delta_c|} \ll |\Delta'| \ll |\Delta_c|$  ( $\Delta_c \Delta' < 0$ ), in view of Eq. (5.1b).

Consider now the dip-bottom shape in the interval between the one- and two-photon resonances, at a sufficient separation from them, defined by the simultaneous inequalities

$$\Delta \Delta' < 0, \quad |\Delta| \gg \sqrt{V_0^2 \nu / |\Delta_c|}, \Gamma, \quad |\Delta'| \gg \sqrt{V_0^2 \nu / |\Delta_c|}, \Gamma'. \quad (5.11)$$

In particular, in the parts of the interval (5.11) defined by the inequalities  $\sqrt{V_0^2 \nu / |\Delta_c|} \ll |\Delta| \ll |\Delta_c|$  and  $\sqrt{V_0^2 \nu / |\Delta_c|} \ll |\Delta'| \ll |\Delta_c|$  one can use the solutions (4.9) and (4.13) with  $|a|, |a_0| \gg 1$ . In view of Eqs. (5.1a) and (5.1b), this yields corrections to the static result proportional to  $a^{-2}$  or  $a_0^{-2}$ —i.e., linear in  $\nu$ . The solutions (4.9) and (4.13) were obtained by means of an omission of some terms proportional to  $\nu$  in Eqs. (4.3) and, as a result, have a limited validity. To describe the spectrum in the whole interval (5.11) one needs the solution of Eqs. (4.3) up to first order in  $\nu$ —i.e., Eq. (4.30):

$$\bar{A}(\Delta) = \frac{1}{V_0^2} \left( \Gamma' \ln \frac{C_2 V_0^2}{|\Delta \Delta'|} + \frac{\Gamma |\Delta'|}{|\Delta|} \right) + \bar{A}_1(\Delta). \quad (5.12a)$$

This line shape is a superposition of the static result (3.16) and a  $\nu$ -dependent term  $\bar{A}_1(\Delta) = \bar{A}_d(\Delta)$  given by Eq. (4.28a):

$$\bar{A}_1(\Delta) = \frac{2\nu}{3|\Delta \Delta'|} + \frac{\nu}{3\Delta^2}. \quad (5.12b)$$

Thus, due to temporal fluctuations, the absorption at the dip bottom increases linearly with  $\nu$ . It is remarkable that the  $\nu$ -dependent term (5.12b) in the spectrum is independent of the field strength  $V_0$ .

## 2. RIT2

The dip-bottom line shape (5.12a) has qualitatively different forms in the cases  $\Gamma' \ll \Gamma$  and  $\Gamma' \gg \Gamma$ . In the latter case for sufficiently small  $\nu$  the dip minimum is close to the static value (3.16), whereas the minimum absorption coefficient is

$$\bar{A}(\Delta_m) \sim \Gamma' / V_0^2 + \nu / \Delta_c^2 \quad (5.13)$$

[cf. Eqs. (3.20), (5.12a), and (5.12b)]. Thus, the line shape of the dip bottom is approximately quasistatic for

$$V_0^2 \nu \ll \Gamma' \Delta_c^2 \quad (5.14)$$

and depends appreciably on  $\nu$  for  $V_0^2 \nu \gg \Gamma' \Delta_c^2$ .

In the case  $\Gamma' \ll \Gamma$  the dip is highly asymmetric. An analysis of Eq. (5.12a) yields that the position of the absorption minimum is close to the two-photon resonance,

$$\Delta_m = -\Delta_c + \Delta_c \frac{\Gamma'}{2\Gamma} \left( 1 + \sqrt{1 + \frac{8\Gamma V_0^2 \nu}{3\Gamma'^2 \Delta_c^2}} \right), \quad (5.15)$$

which holds until  $|\Delta_m + \Delta_c| \ll |\Delta_c|$ —i.e., for

$$\sqrt{V_0^2 \nu} \ll |\Delta_c| \sqrt{\Gamma}. \quad (5.16)$$

The absorption coefficient at the minimum  $\bar{A}(\Delta_m)$  is obtained by setting in Eq. (5.12a)  $\Delta' = \Delta_m + \Delta_c$  and  $\Delta \approx \Delta_c$ . For

$$V_0^2 \nu \ll \Gamma'^2 \Delta_c^2 / \Gamma, \quad (5.17)$$

the quantities  $\Delta_m$  [Eq. (5.15)] and  $\bar{A}(\Delta_m)$  reduce to their quasistatic values (3.22) and (3.23).

However, for  $V_0^2 \nu \gg \Gamma'^2 \Delta_c^2 / \Gamma$  the spectral minimum significantly depends on  $\nu$ . In particular, in the interval

$$|\Delta_c| \Gamma' / \sqrt{\Gamma} \ll \sqrt{V_0^2 \nu} \ll |\Delta_c| \sqrt{\Gamma}, \quad (5.18)$$

the minimum position shifts towards the one-photon resonance  $\Delta=0$  with an increase of the field intensity and/or bandwidth, according to the expression

$$\Delta_m = \Delta_c \left[ -1 + \sqrt{2V_0^2 \nu / (3\Gamma \Delta_c^2)} \right], \quad (5.19)$$

whereas the minimum value increases with  $\nu$  as  $\sqrt{\nu}$ :

$$\bar{A}(\Delta_m) = \frac{\sqrt{8\Gamma \nu / 3}}{V_0 |\Delta_c|}. \quad (5.20)$$

The sharp asymmetry, which characterizes the line shape in the quasistatic regime (see Sec. III), is smoothed out with the increase of  $\nu$ : however in the interval (5.18) the line shape still remains highly asymmetric.

Though in the region (5.18) the absorption minimum is determined by the  $\nu$ -dependent term (5.12b) [cf. Eqs. (5.19) and (5.20)], the dip line shape (5.12a) and (5.12b) as a whole is not completely dominated by the term  $\bar{A}_1(\Delta)$ . To find under which condition  $\bar{A}_1(\Delta)$  dominates in Eq. (5.12a) (for an arbitrary relation between  $\Gamma$  and  $\Gamma'$ ), consider typical values of  $\Delta, |\Delta| \sim |\Delta'| \sim |\Delta_c|$ . Then Eq. (5.12a) yields  $\bar{A}(\Delta) \sim (\Gamma + \Gamma') / V_0^2 + \nu / \Delta_c^2$ . The latter relation implies that the dip line shape is described in the first approximation by Eq. (5.12b) when the bandwidth  $\nu$  and/or the coupling amplitude  $V_0$  are sufficiently large:

$$V_0^2 \nu \gg (\Gamma + \Gamma') \Delta_c^2. \quad (5.21)$$

The line shape (5.12b) is a somewhat asymmetric dip with the shape independent of  $\nu$ . The minimum of the dip is located at

$$\Delta_m = -\frac{\sqrt{5}-1}{2} \Delta_c \approx -0.618 \Delta_c, \quad (5.22)$$

which is the *golden section of the interval between the one- and two-photon resonances*. The minimum value is

$$\bar{A}(\Delta_m) = \frac{11 + 5\sqrt{5}}{6} \frac{\nu}{\Delta_c^2} \approx 3.70 \frac{\nu}{\Delta_c^2}. \quad (5.23)$$

Consider now the RIT2 validity conditions. As mentioned above, for a very small reservoir bandwidth  $\nu$ , RIT2 is guaranteed under the condition (3.27). With an increase of the bandwidth  $\nu$  the minimal absorption increases; hence, an additional RIT2 validity condition involving  $\nu$  should appear. The latter is obtained by inserting Eqs. (5.22) and (5.23) into Eq. (3.25), yielding the condition

$$\nu \ll \Gamma. \quad (5.24)$$

Note that, until  $V_0^2 \ll |\Delta_c|^3/\Gamma$ , the inequality (5.24) is stricter than the validity condition (4.7) of the present theory.

When the bandwidth  $\nu$  is so large that condition (4.7) is violated, the probe-absorption coefficient does not change significantly over the spectral interval between one- and two-photon resonances (see Sec. V B), and there remains only one important RIT frequency—viz., the probe resonance (RIT1).

### B. Broadband (quasiresonant) field

In the case of a broadband field,

$$(V_0^2 \nu)^{2/3} \gg \Delta_c^2, \quad (5.25)$$

$\Delta_c$  can be considered as a small parameter, and, as the first approximation, one can use the results obtained for the resonant-field case [32,33].

#### 1. Strong coupling

When the coupling is strong or moderate,  $V_0 \gtrsim \nu$ , one can neglect the material constants in Eqs. (4.3). Though the resulting equations cannot be solved analytically, one can obtain that, in the limit of a strong coupling,

$$\Delta_c^2 \ll (V_0^2 \nu)^{2/3} \ll V_0^2, \quad (5.26)$$

the spectrum still consists of two peaks. RIT1 is well described by the result [32]

$$\bar{A}(0) \approx 1.728 \frac{\nu^{1/3}}{V_0^{4/3}} \quad (5.27)$$

obtained for the resonant case  $\Delta_c=0$  (see numerical calculations in Sec. V E). The spectrum  $\bar{A}(\Delta)$  is close to the value (5.27) in the spectral interval  $|\Delta| \ll (V_0^2 \nu)^{1/3}$ , the minimum occurring for the probe frequency between the one- and two-photon resonances (see Sec. V E). For greater detunings one can obtain from Eqs. (4.30) and (4.28a) a correction to the static result (3.8):

$$\bar{A}(\Delta) \approx \frac{\pi|\Delta'|}{V_0^2} - \frac{\nu}{3\Delta'^2} \quad [(V_0^2 \nu)^{1/3} \ll |\Delta| \ll V_0]. \quad (5.28)$$

Note that for  $\Delta_c=0$ , Eq. (5.28) reduces to the result (5.8) and (5.9) in Ref. [32], obtained by a different method.

#### 2. Weak coupling

With the increase of the bandwidth, the hole depth decreases, until at  $\nu \sim V_0$  the dip vanishes and the spectrum becomes a single broad, slightly asymmetric peak. In the weak-coupling case  $\nu \gg V_0$ , the main part of the spectrum becomes a Lorentzian centered at the one-photon resonance with the width decreasing with  $\nu$  [33]:

$$\bar{A}(\Delta) = \frac{\Gamma + V_0^2/\nu}{(\Gamma + V_0^2/\nu)^2 + \Delta^2} \quad (|\Delta| \ll \nu). \quad (5.29)$$

Finally, as follows from Eq. (5.29), for a very large bandwidth  $\nu \gg V_0^2/\Gamma$ , the probe spectrum approaches the line

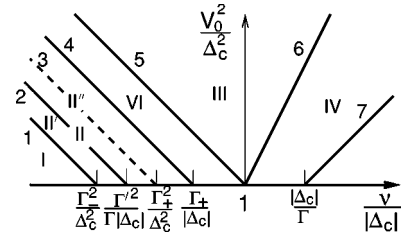


FIG. 2. The log-log plot of the boundaries (thick solid lines) of different regimes (denoted by roman numerals) in the parameter space, with  $\Gamma_+ = \max\{\Gamma, \Gamma'\}$  and  $\Gamma_- = \min\{\Gamma, \Gamma'\}$ . Boundary 2 exists only in the case  $\Gamma \gg \Gamma'$ .

shape with the vanishing control field, Eq. (3.26).

### C. Spectral wings

The spectral wings for an arbitrary  $\nu$  follow from the cumulant expansion (see Eq. (4.14) in [33]),

$$\bar{A}(\Delta) = \frac{\Gamma}{\Delta^2} + \frac{V_0^2(\Gamma' + \nu)}{\Delta^4} \quad (|\Delta| \gg V_0, \nu), \quad (5.30)$$

which is an extension of Eq. (3.17). As follows from Eq. (5.30), the spectral wings appreciably depend on the bandwidth  $\nu$  when both  $\nu \gg \Gamma$  and  $\nu \gtrsim \Gamma'$ .

Alternatively, the result (5.30) can be obtained from Eqs. (4.23) and (4.24), on taking into account that the inequality  $|\Delta| \gg V_0$  is equivalent to  $|b| \gg 1$ , in view of Eq. (2.6), and on using Eq. (4.26b). Note that the summands resulting from the term  $L_0 \Psi_a$  in Eq. (4.3) [cf. the remark after Eq. (4.26b)] cancel in the derivation of Eq. (5.30). Hence, the solution (4.10), unlike Eq. (4.5), describes correctly the wings (5.30).

### D. Separation of the situations

To summarize the above results, consider the transformation of the probe spectrum with the increase of the bandwidth for a fixed control-field intensity. Figure 2 shows the boundaries of different regimes of the behavior of an atom coupled to a high-temperature Lorentzian reservoir (or Gaussian-Markovian amplitude-phase fluctuating field) for an off-resonant, strong coupling [we consider only the upper half plane in Fig. 2, in accordance with condition (2.6)]. When the control field has a very narrow bandwidth, so that the both conditions (5.2) hold (region I in Fig. 2), the spectrum shape is quasistatic (see Sec. III). Between boundaries 1 and 7 in Fig. 2 the line shape significantly depends on  $\nu$ . In particular, for  $\Gamma < \Gamma'$  ( $\Gamma > \Gamma'$ ) the one-photon (two-photon) edge of the spectral dip is described by Eq. (5.4) [Eq. (5.9)] in regions II and VI in Fig. 2, whereas the other edge is given by Eq. (5.9) [Eq. (5.4)] in the area between lines 3 and 5. In regions I and II the dip bottom depends on material relaxation and hence on quantum interference. The dip bottom remains mainly static in region II (i.e., between lines 1 and 4) for  $\Gamma \leq \Gamma'$  or in region II' for  $\Gamma \gg \Gamma'$  (strong destructive interference). In the latter case in region II' [Eq. (5.18)] the line shape depends on  $\nu$  in a vicinity of the spectral minimum [Eqs. (5.19) and (5.20)]. In regions VI and III in Fig. 2 the line shape is independent of material relaxation [except

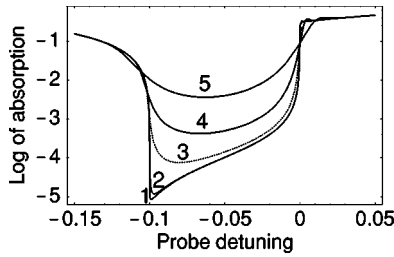


FIG. 3.  $\log_{10}\bar{A}(\Delta)$  as a function of  $\Delta$  for  $V_0=1$ ,  $\Delta_c=0.1$ ,  $\Gamma=10^{-4}$ ,  $\Gamma'=10^{-6}$ , and  $\nu=0$  (curve 1),  $\nu=10^{-9}$  (curve 2),  $\nu=10^{-7}$  (curve 3),  $\nu=10^{-6}$  (curve 4), and  $\nu=10^{-5}$  (curve 5). Curve 2 corresponds to region II'' and line 3 in Fig. 2, curve 3 corresponds to region II'', curve 4 corresponds to boundary 4, and curve 5 corresponds to region VI.

for far wings, Eq. (5.30)]. In particular, in region VI [conditions (4.7) and (5.21)] the dip-bottom line shape is proportional to  $\nu$ , being independent of the control-field intensity [Eq. (5.12b)], whereas in region III [Eq. (5.26)] the broadband, strong-coupling regime holds [Eqs. (5.27) and (5.28)]. In region IV the coupling is weak and the spectrum is given by the single peak (5.29), whereas to the right of boundary 7 the control field is so broadband that it does not affect the unperturbed spectrum (3.26).

**E. Numerical results and discussion**

For numerical calculations we have used an exact solution in the form of the continued fraction [33]

$$\bar{A}(\Delta) = \text{Re}(\tilde{\Gamma} + D_1)^{-1}, \tag{5.31a}$$

where  $(n=1,2,\dots)$

$$D_n = \frac{nV_0^2}{\tilde{\Gamma}' + (2n-1)\nu + nV_0^2/(\tilde{\Gamma} + 2n\nu + D_{n+1})}. \tag{5.31b}$$

The convergence of the continued fraction (5.31a) and (5.31b) sharply worsens with the decrease of  $\nu$ , leading to extensive computational times for sufficiently small  $\nu$ . Therefore for very small  $\nu$  we performed numerical calculations by the formulas (3.2), (4.5), and (4.10), which allow for fast calculations for any  $\nu$  and have been verified, by a com-

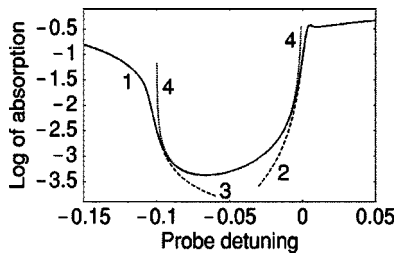


FIG. 4.  $\log_{10}\bar{A}(\Delta)$  as a function of  $\Delta$  for  $V_0=1$ ,  $\Delta_c=0.1$ ,  $\Gamma=10^{-4}$ ,  $\Gamma'=10^{-6}$ , and  $\nu=10^{-6}$  (curve 1). For comparison, we plot approximate results: curve 2, Eq. (5.4); curve 3, Eq. (5.9); curve 4, Eq. (5.12a) and (5.12b).

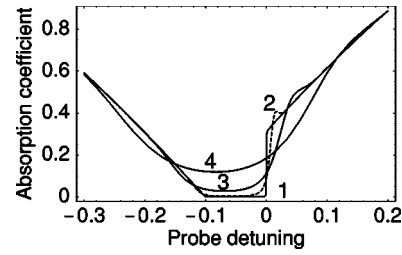


FIG. 5. The absorption coefficient  $\bar{A}(\Delta)$  as a function of  $\Delta$  for  $V_0=1$ ,  $\Delta_c=0.1$ ,  $\Gamma=10^{-4}$ ,  $\Gamma'=10^{-6}$ , and  $\nu=0$  (curve 1),  $\nu=10^{-5}$  (curve 2),  $\nu=10^{-4}$  (curve 3), and  $\nu=10^{-3}$  (curve 4). Curves 2 and 3 correspond to region VI and curve 4 corresponds to boundary 5 in Fig. 2.

parison with Eq. (5.31a) and (5.31b), to yield very accurate results in their validity regions obtained above.

Figures 3–6 show the transformation of the probe spectrum with an increase of the control-field bandwidth  $\nu$ , the other parameters being fixed. The static-limit curves 1 in Figs. 3, 5, and 6 were plotted by Eq. (3.2). The “exact” curves for nonvanishing  $\nu$  were plotted by Eq. (5.31a) and (5.31b), except for the plots with  $\nu < 10^{-6}$  (curves 2 and 3 in Fig. 3) obtained by using Eqs. (3.2), (4.5), and (4.10) in intervals of their validity [see the remark after Eq. (5.31a) and (5.31b)]. In Figs. 3–6 we concentrate on the case of strong destructive interference ( $\Gamma \gg \Gamma'$ ), which is favorable for RIT. Curve 1 in Fig. 3 shows the static shape of the spectral dip, which is highly asymmetric, the minimum being near the two-photon resonance [see Eqs. (3.22) and (3.23)].

As shown in Figs. 3–6, absorption at the spectral minimum increases with  $\nu$ . The position of the minimum in Fig. 3 shifts with  $\nu$  toward the one-photon resonance, as expected for region II'' [see Eqs. (5.15) and (5.20)]. Figure 4 shows curve 4 of Fig. 3 together with approximate formulas (5.4), (5.9), (5.12a), and (5.12b). It demonstrates that the above formulas hold in overlapping spectral intervals and allow together for a rather accurate description of the spectral dip in regions II and VI. The extra peak near the one-photon resonance can be seen in Figs. 3 (curves 3–5) and 5 (curve 2). The extra peak shifts and broadens with  $\nu$  approximately as  $\sqrt{\nu}$  [see Eqs. (5.4) and (5.6)]. When  $\nu$  increases so that inequality (4.7) becomes not too strong, the local maximum

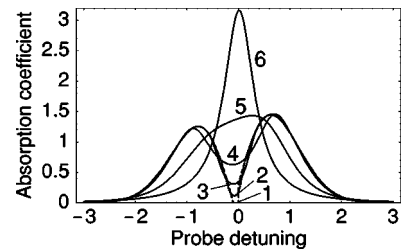


FIG. 6. The absorption coefficient  $\bar{A}(\Delta)$  as a function of  $\Delta$  for  $V_0=1$ ,  $\Delta_c=0.1$ ,  $\Gamma=10^{-4}$ ,  $\Gamma'=10^{-6}$ , and  $\nu=0$  (curve 1),  $\nu=10^{-3}$  (curve 2),  $\nu=0.01$  (curve 3),  $\nu=0.1$  (curve 4),  $\nu=1$  (curve 5), and  $\nu=3$  (curve 6). Curves 2 and 5 correspond to boundaries 5 and 6 in Fig. 2, respectively, curves 3 and 4 correspond to region III, and curve 6 corresponds to region IV.

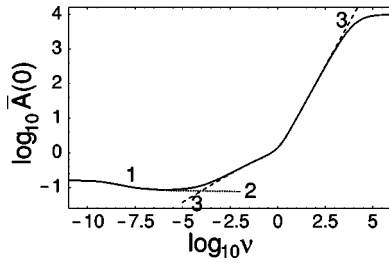


FIG. 7. Dependence of the resonance absorption  $\bar{A}(0)$  on the field bandwidth  $\nu$  in the log-log scale (curve 1), with  $V_0=1$ ,  $\Delta_c=0.1$ , and  $\Gamma=\Gamma'=10^{-4}$ . For comparison, we show the analytical result (4.5) (curve 2) and the numerical solution obtained for  $\Delta_c=\Gamma=\Gamma'=0$  [32] (curve 3).

disappears (see curve 3 in Fig. 5), since the analytic solution (4.5) and the ensuing equations, (5.4)–(5.6) become not exact. Figure 6 shows the line shape for sufficiently large  $\nu$ . As demonstrated by Fig. 6, in region III the line shape changes weakly in the interval between one- and two-photon resonances, the spectral minimum occurring in the latter interval. Absorption at the minimum increases with the increase of  $\nu$ , until at  $\nu \sim V_0$  the spectral dip disappears and the spectrum becomes a single slightly asymmetric, broad peak (curve 5 in Fig. 6). With the further increase of  $\nu$  the spectrum becomes a symmetric Lorentzian peak [curve 6 in Fig. 6, Eq. (5.29)], the height of which increases and the width decreases, until it approaches the unperturbed line shape (3.26).

The dependence of the resonance absorption (i.e., RIT1) on the control-field bandwidth  $\nu$  is shown in Fig. 7 (curve 1). Note a counterintuitive fact of a decrease of absorption with respect to the static value by approximately a half [cf. Eq. (5.7)], which holds in regions II and VI ( $10^{-9} \ll \nu \ll 10^{-3}$  in Fig. 7). A comparison of curves 1 and 2 in Fig. 7 shows that analytic formula (4.5) describes well the resonant absorption in case (4.7) (regions I, II, and VI), whereas a comparison of curves 1 and 3 reveals that the result for the resonant absorption (RIT1) with a *resonant* control field obtained in Ref. [32] approximates very well the present case of a off-resonant control field when the bandwidth is sufficiently broad [Eq. (5.25)—i.e., regions III and IV]. Note that curve 3 in Fig. 7 has two linear asymptotes: the small- $\nu$  one, Eq. (5.27), and the large- $\nu$  one,  $\bar{A}(0)=\nu/V_0^2$ , implied by Eq. (5.29) with a negligible  $\Gamma$ . For very large  $\nu$  curve 1 in Fig. 7 tends to a constant corresponding to the unperturbed line, in compliance with Eq. (5.29).

## VI. CONCLUSION

In the present paper we have provided a comprehensive analytic treatment of the spectrum of weak-probe-field absorption affected by a strong, off-resonant coupling of an adjacent atomic transition to a high-temperature Lorentzian bosonic reservoir or to chaotic laser light. Furthermore, we have made a detailed analysis of reservoir-induced transpar-

ency, especially for resonance (RIT1) and off-resonance (RIT2) types of it. The formulas obtained have been shown to provide readily numerical results for very small reservoir widths  $\nu$ , when the existing numerical methods are ineffective. We have revealed two unexpected spectral features, which are induced by temporal fluctuations of the control field in certain ranges of the values of the bandwidth  $\nu$ : an *increase* of RIT1 with  $\nu$  and an *extra peak* near the probe resonance. These remarkable features are properties of the peculiar line shape (5.4), which emerges in a vicinity of the one-photon resonance due to diffusion of the complex amplitude.

It is noteworthy that the above unexpected spectral features are specific to the present statistical model of control-field temporal behavior. Indeed, they can be shown to be absent for an uncorrelated-jump [30] control field, which has the same amplitude distribution (3.1) and the spectrum (4.1) as the chaotic field considered here.

## ACKNOWLEDGMENT

The present research was supported by the Ministry of Absorption via the Center for Absorption of Scientists.

## APPENDIX: VALIDITY CONDITIONS OF THE ANALYTICAL SOLUTIONS (4.5) AND (4.10)

Necessary conditions for the validity of Eqs. (4.5) and Eq. (4.10), respectively, are [33]

$$\sqrt{V_0^2\nu} \ll (\Gamma' + |\Delta'|)(\sqrt{\Gamma + |\Delta|} + \sqrt{\Gamma' + |\Delta'|}), \quad (\text{A1a})$$

$$\nu \ll \Gamma' + |\Delta'|, \quad (\text{A1b})$$

and [30]

$$\sqrt{V_0^2\nu} \ll (\Gamma + |\Delta|)(\sqrt{\Gamma + |\Delta|} + \sqrt{\Gamma' + |\Delta'|}), \quad (\text{A2a})$$

$$\nu \ll \Gamma + |\Delta|. \quad (\text{A2b})$$

Consider the dip region (3.5), where the most interesting modification of the spectrum occurs. As noted after Eq. (5.11), in this region, except for narrow vicinities of one- and two-photon resonances, the solutions (4.5) and (4.10) provide small corrections to the static result and thus overlap with the approximate solution (4.30). The first-order corrections provided by Eqs. (4.5) and (4.10) are given by the second and first terms in Eq. (4.28a), respectively [cf. the remark after Eq. (4.26a) and (4.26b)]. Hence, if the solutions (4.5) and (4.10) hold in the interval (3.5), then  $|\tilde{\Gamma}| \ll |\tilde{\Gamma}'|$  and  $|\tilde{\Gamma}| \gg |\tilde{\Gamma}'|$ , respectively. On the account of Eq. (2.6), this means that inside the spectral region (3.5) the solutions (4.5) and (4.10) hold in the intervals (4.8) and (4.12), respectively. Note that in these intervals the conditions (A1a) and (A2a) are equivalent to Eq. (4.7), whereas conditions (A1b) and (A2b) reduce to  $\nu \ll |\Delta_c|$ . The latter inequality is weaker than Eq. (4.7), in view of Eq. (2.6).

- [1] M. A. Nielsen and I. L. Chuang, *Quantum Computation and Quantum Information* (Cambridge University Press, Cambridge, England, 2000); P. Zanardi and M. Rasetti, Phys. Rev. Lett. **79**, 3306 (1997); D. A. Lidar, I. L. Chuang, and K. B. Whaley, *ibid.* **81**, 2594 (1998); G. S. Agarwal, Phys. Rev. A **61**, 013809 (1999); G. S. Agarwal, M. O. Scully, and H. Walther, *ibid.* **63**, 044101 (2001); Phys. Rev. Lett. **86**, 4271 (2001); L. Viola and S. Lloyd, Phys. Rev. A **58**, 2733 (1998); D. Vitali and P. Tombesi, *ibid.* **65**, 012305 (2001); A. G. Kofman and G. Kurizki, Phys. Rev. Lett. **93**, 130406 (2004); **87**, 270405 (2001); Nature (London) **405**, 546 (2000).
- [2] C. P. Slichter, *Principles of Magnetic Resonance* (Springer, Berlin, 1978); C. W. Gardiner, *Quantum Noise* (Springer, Berlin, 1991).
- [3] C. Cohen-Tannoudji, J. Dupont-Roc, and G. Grynberg, *Atom-Photon Interactions* (Wiley, New York, 1992).
- [4] M. O. Scully and M. S. Zubairy, *Quantum Optics* (Cambridge University Press, Cambridge, England, 1997).
- [5] A. J. Leggett, S. Chakravarty, A. T. Dorsey, M. P. A. Fisher, A. Garg, and W. Zwerger, Rev. Mod. Phys. **59**, 1 (1987).
- [6] A. G. Kofman, G. Kurizki, and B. Sherman, J. Mod. Opt. **41**, 353 (1994).
- [7] U. Fano, Phys. Rev. **124**, 1866 (1961).
- [8] B. Fain, Phys. Rev. A **37**, 546 (1988).
- [9] M. A. Krivoglaz, Zh. Eksp. Teor. Fiz. **48**, 310 (1965) [Sov. Phys. JETP **21**, 204 (1965)].
- [10] I. S. Osad'ko, in *Spectroscopy and Excitation Dynamics of Condensed Molecular Systems*, edited by V. M. Agranovich and R. M. Hochstrasser (North-Holland, Amsterdam, 1983), p. 437.
- [11] Zero-phonon line shapes of impurities in solids are of a current interest in studies of, e.g., tunable laser crystals [M. Dong-ping and Z. Ji-ping, Phys. Rev. B **68**, 054111 (2003)] and polymers [I. Renge, Chem. Phys. Lett. **377**, 286 (2003)].
- [12] J. J. Childs, K. An, M. S. Otteson, R. R. Dasari, and M. S. Feld, Phys. Rev. Lett. **77**, 2901 (1996); R. J. Thompson, Q. A. Turchette, O. Carnal, and H. J. Kimble, Phys. Rev. A **57**, 3084 (1998).
- [13] F. Bernardot, P. Nussenzeveig, M. Brune, J. M. Raimond, and S. Haroche, Europhys. Lett. **17**, 33 (1992).
- [14] A. Auffeves, P. Maioli, T. Meunier, S. Gleyzes, G. Nogues, M. Brune, J. M. Raimond, and S. Haroche, Phys. Rev. Lett. **91**, 230405 (2003).
- [15] A. Y. Smirnov, L. G. Murokh, and N. J. M. Horing, Physica E (Amsterdam) **19**, 58 (2003).
- [16] P. Dahan and I. D. Vagner, Physica B **346-347**, 465 (2004).
- [17] J. I. Cirac, H. Ritsch, and P. Zoller, Phys. Rev. A **44**, 4541 (1991).
- [18] A. G. Kofman, Phys. Rev. A **64**, 033809 (2001).
- [19] H. M. Sevian and J. L. Skinner, J. Chem. Phys. **91**, 1775 (1989); M. Aihara, H. M. Sevian, and J. L. Skinner, Phys. Rev. A **41**, 6596 (1990); H. Risken, L. Schoendorff, and K. Vogel, *ibid.* **42**, 4562 (1990).
- [20] J. J. Sanchez-Mondragon, N. B. Narozhny, and J. H. Eberly, Phys. Rev. Lett. **51**, 550 (1983); G. S. Agarwal, *ibid.* **53**, 1732 (1984); M. G. Raizen, R. J. Thompson, R. J. Brecha, H. J. Kimble, and H. J. Carmichael, *ibid.* **63**, 240 (1989).
- [21] J. E. Field, Phys. Rev. A **47**, 5064 (1993).
- [22] A. G. Kofman and G. Kurizki, Opt. Commun. **153**, 251 (1998).
- [23] Lasing without inversion induced by a classical coherent field was discussed in Ref. [4]; O. Kocharovskaya, Phys. Rep. **219**, 175 (1992); M. O. Scully, *ibid.* **219**, 191 (1992); P. Mandel, Contemp. Phys. **34**, 235 (1993); see special issue of Quantum Opt. **6**, 201 (1994); G. G. Padmabandu, G. R. Welch, I. N. Shubin, E. S. Fry, D. E. Nikonov, M. D. Lukin, and M. O. Scully, Phys. Rev. Lett. **76**, 2053 (1996); P. B. Sellin, G. A. Wilson, K. K. Meduri, and T. W. Mossberg, Phys. Rev. A **54**, 2402 (1996).
- [24] A. I. Burshtein and A. G. Kofman, Zh. Eksp. Teor. Fiz. **70**, 840 (1976) [Sov. Phys. JETP **43**, 436 (1977)]; P. Avan and C. Cohen-Tannoudji, J. Phys. B **10**, 155 (1977); A. T. Georges and P. Lambropoulos, Phys. Rev. A **20**, 991 (1979); P. Zoller, *ibid.* **20**, 2420 (1979); **20**, 1019 (1979); A. I. Burshtein and A. Y. Sivachenko, J. Nonlinear Opt. Phys. Mater. **5**, 833 (1996).
- [25] G. Vemuri, K. V. Vasavada, and G. S. Agarwal, Phys. Rev. A **52**, 3228 (1995).
- [26] Note also studies of effects of phase-fluctuating fields (with a Lorentzian spectrum) on quantum systems: A. I. Burshtein, Zh. Eksp. Teor. Fiz. **49**, 1362 (1965) [Sov. Phys. JETP **22**, 939 (1966)]; G. S. Agarwal, Phys. Rev. Lett. **37**, 1383 (1976); J. H. Eberly, *ibid.* **37**, 1387 (1976); J. H. Eberly, K. Wódkiewicz, and B. W. Shore, Phys. Rev. A **30**, 2381 (1984); A. G. Kofman, R. Zaibel, A. M. Levine, and Y. Prior, *ibid.* **41**, 6434 (1990); **41**, 6454 (1990) and references therein.
- [27] L. D. Zusman and A. I. Burshtein, Zh. Eksp. Teor. Fiz. **61**, 976 (1971) [Sov. Phys. JETP **34**, 520 (1972)].
- [28] S. G. Przhibelskii, Opt. Spektrosk. **35**, 715 (1973) [Opt. Spectrosc. **35**, 415 (1973)]; P. V. Elyutin, *ibid.* **43**, 542 (1977) [ **43**, 318 (1977)].
- [29] N. F. Perelman, I. Sh. Averbukh, and V. A. Kovarsky, Zh. Eksp. Teor. Fiz. **93**, 483 (1987) [Sov. Phys. JETP **66**, 276 (1987)].
- [30] A. G. Kofman, Phys. Rev. A **56**, 2280 (1997).
- [31] A. G. Kofman, Europhys. Lett. **46**, 164 (1999).
- [32] A. G. Kofman, Phys. Rev. A **63**, 033810 (2001).
- [33] A. G. Kofman, Eur. Phys. J. D **17**, 153 (2001); **21**, 121(E) (2002).
- [34] K.-J. Boller, A. Imamoglu, and S. E. Harris, Phys. Rev. Lett. **66**, 2593 (1991); Y. Q. Li and M. Xiao, Phys. Rev. A **51**, 4959 (1995); S. E. Harris, Phys. Today **50**(7), 36 (1997).
- [35] J. E. Field, K. H. Hahn, and S. E. Harris, Phys. Rev. Lett. **67**, 3062 (1991).
- [36] F. S. Cataliotti, C. Fort, T. W. Hänsch, M. Inguscio, and M. Prevedelli, Phys. Rev. A **56**, 2221 (1997); S. Scandolo and F. Bassani, Phys. Rev. B **45**, 13 257 (1992).
- [37] S. H. Autler and C. H. Townes, Phys. Rev. **100**, 703 (1955).
- [38] *Handbook of Mathematical Functions*, Natl. Bur. Stand. Appl. Math. Ser. No. 55, edited by M. Abramowitz and I. A. Stegun (U.S. GPO, Washington, DC, 1964).
- [39] In this derivation we used the equality  $E_1(-x \pm i0) = -\text{Ei}(x) \mp \pi\theta(x)$  ( $x > 0$ ), where  $\text{Ei}(x)$  is an integral exponential function [see Eqs. (5.1.2) and (5.1.7) in [38]].
- [40] G. S. Agarwal and G. Vemuri, Phys. Rev. A **55**, 1466 (1997).